Journal of Hydroscience and Hydraulic Engineering
Vol. 1, No. 1, April, 1983, pp.75-82.

TURBULENT STRUCTURE WITH LONGITUDINAL SECONDARY FLOW

By

Hiroji Nakagawa

Dept. of Civil Engrg., Kyoto University, Kyoto, Japan

Iehisa Nezu

Dept. of Civil Engrg., Kyoto University, Kyoto, Japan

and

Akihiro Tominaga

Dept. of Civil Engrg., Gunma University, Kiryu, Gunma, Japan

SYNOPSIS

In actual river stream, the existence of longitudinal cellular secondary flow is recognized and it plays an important role in sediment transport, river bed formation and diffusion process. In this study, the turbulent structures of the flow with secondary flow in straight channel with a rectangular cross section are investigated by stimulating the occurrence of the secondary flow artificially. Because the velocity of secondary flow is usually within 4 percents of the main flow velocity, the experiments were conducted in air duct flow which is considered to be similar to open channel flow except the presence of free surface. The mean velocity, the turbulence intensity and the Reynolds stress in the region including one secondary flow cell were measured, and the internal structure of the flow is briefly discussed on the basis of the equation of motion. It has been shown that the secondary flow considerably changes the turbulent structures and the transverse Reynolds stress $-\overline{uw}$ widely undulates.

INTRODUCTION

Several river engineers have reported the existence of spanwise bed structures such as sand ribbons or sand ridges which consist of alternating ridges and broad hollows aligned parallel to the mean flow (see e.g. (1), (2)). These spanwise structures suggest the occurrence of the longitudinal cellular secondary flow characterized by a pair of counter-rotating streamwise vortices of which diameter is nearly equal to the flow depth, and these are seemed to be caused by initially existing secondary flow. On the contrary, it may be true that these structures develop and maintain the secondary flow. The present study is to investigate the interrelation between these spanwise bed structures and the cellular secondary flow and to make clear the turbulent structures of the flow with the secondary flow.

Previously, the authors conducted an experiment under a bed configuration in which the longitudinal and alternate stripes of smooth and rough beds were set spanwisely and showed that in favorable condition there appeared an evident secondary flow which is downflow on the rough bed and upflow on the smooth bed (3). After that, the authors made an experiment under a bed condition in which longitudinal roughness elements were attached onto the channel bed for simulating sand ridges. In this case, an upflow was produced on the ridge while a downflow appeared on the trough (4). In these two experiments, the flow has not developed enough because the distance from the entrance to the test section was too short and the roughness elements were attached to the lower bed only. In this study, therefore, these defects have been improved and the flow properties in yhe area between the ridge and the trough have been measured in detail. It is difficult to measure the secondary flow, because their velocity is usually within 4 percents of the main flow velocity. Thus, the present experiment has been performed in air duct flow in the same manner as the previous two experiments.

EXPERIMENTAL PROCEDURE

Experiments were conducted in a straight channel 6m long with a rectangular closs section of 8cm x 18cm. Air was supplied to channel by a centrifugal fan through a 40cm-square settling chamber of 140cm in length and contracting section of 60cm in length. In order to promote the the developemement of flow, the rough sand-papers were attached onto both the lower and the upper walls at the entrance of the channel and the test section was set up at 4.75m downstream from its entrance.

Experiment was first conducted on a uniform smooth bed (CASE-H). Next, in order to simulate the afore mentioned sand ridges, 6m long roughness elements with trapezoidal cross section which had 1cm upper-side width, 2cm lower-side width and 0.5cm height were attached onto both the lower and the upper walls of the channel. Though, the actual river seems not to have such a regular and large bed configulation, these roughness elements were selected in order to emphasize the effects of the ridge. The intervals of roughness elements were selected to be a half of the channel height (=a) in CASE-I and a channel height (=2a) in CASE-J, as shown in Fig. 1 (a) and (b). As the width of a pair of counter-rotating secondary flows in actual rivers is about two times the flow depth, CASE-J seems to be realistic if a half of the channel height could be regarded as the flow depth of open channel flow.

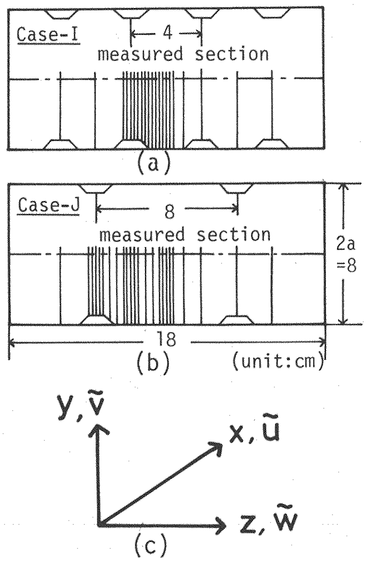

Fig. 1 Test section and coordinate system

The maximum mean flow velocity, U_{max}, was fixed to be about 5m/sec in these three cases. The coordinate system used in this study is shown on Fig. 1(c). The scope of the test section and measured points of CASE-I and CASE-J are shown in Fig. 1(a) and (b), respectively. The velocity measurements were carried out at 15 points in y-direction and at interval of 2 to 4mm in z-direction between ridge and trough($z/a = -0.5$ to 0.0 in CASE-I and $z/a = -1.0$ to 0.0 in CASE-J). Two velocity pairs of $(\tilde{u},\tilde{v})$ and $(\tilde{u},\tilde{w})$ were measured by x-type hot-wires(DISA 55P61). The hot-wire signals were recorded in digital form by using an AD-converter, with sampling size $N = 20,000$ and the sampling frequency $f = 2,000$Hz. Next, some statistical analyses were carried out by a large digital computer at the Data Processing Center, Kyoto University.

EXPERIMENTAL RESULT AND DISCUSSION

Fig. 2 shows the contours of the primary mean velocity U and the turbulence intensity u' in the case of uniform smooth bed CASE-H. Both values are normalized by U_{max}, and in the following all experimental values of velocity will be normalized by U_{max}. Even in case of the uniform smooth boundary, the velocity distribution is distorted and two-dimensionality cannot be maintained. This seems to be due to the secondary flow produced by corner effects. But, because, in the zone $|z/a| < 1$, the vertical mean velocity V is only 0.3 percent of U_{max} and the Reynolds stress $-\overline{uv}$ indicates linear distribution, the secondary flow caused by

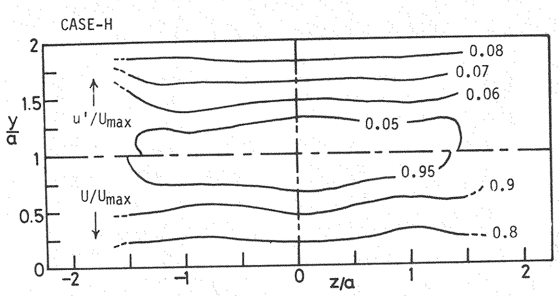

Fig. 2 Contours of primary mean velocity U and turbulence intensity u' on uniform smooth bed (CASE-H)

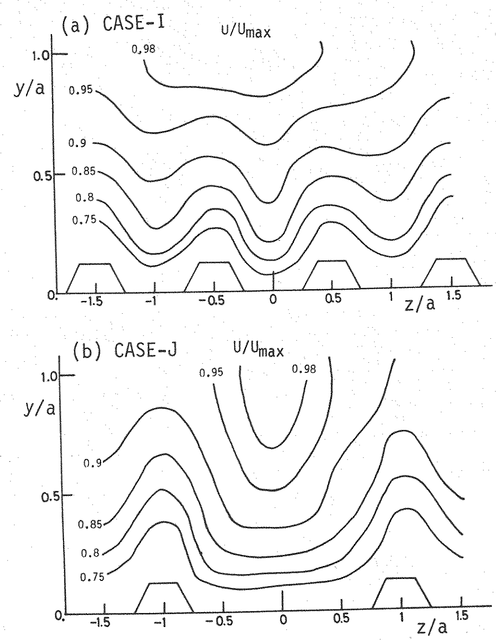

Fig. 3 Contours of primary mean velocity U

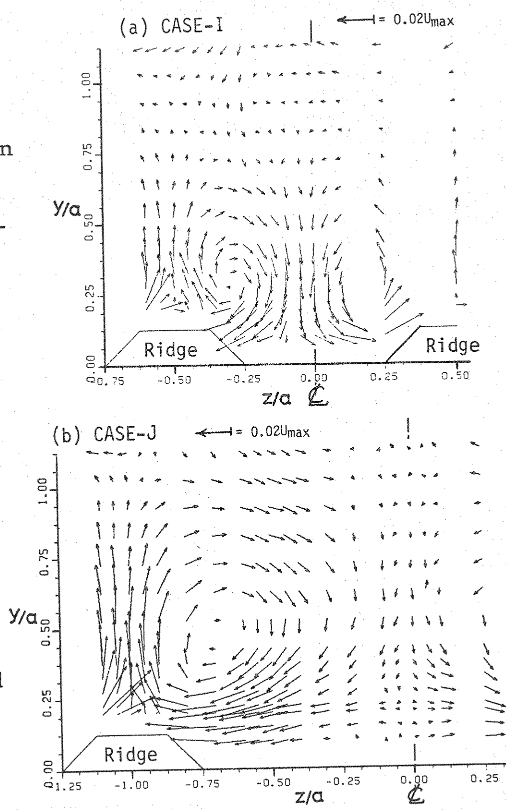

Fig. 4 Secondary flow velocity vectors

corner effects hardly influence the turbulent structures.

As for the cases with roughness elements, Fig. 3(a) and (b) show the contours of U in CASE-I and CASE-J, respectively The value of U undulates transversely so as to be lower on the ridge and higher on the trough. The region on the roughness element is called the ridge area, the region between these elements is called the trough area and the region on the boundary of above two areas is called the boundary area. Though the lateral variation of U of CASE-I becomes smaller as it approaches the center of the channel, that of CASE-J is significantly large even at the center of the channel.

Fig. 4(a) and (b) show the distribution of secondary flow velocity vectors in CASE-I and J, respectively. In both cases, an upflow appears on the ridge area and a downflow on the trough area, and the existence of the secondary flow is verified by this figures. The upflow velocity of CASE-I is almost equal to the downflow velocity and is 2 to 3 % of U_{max}. On the other hand, the upflow velocity of CASE-J is larger(4 % of U_{max}) than the downflow velocity(0.5 to 1 % of U_{max}). But, the width of upflow is narrower than that of downflow, and such a characteristic of strong upflow and weaker downflow over wider region is also recognized in the cellular secondary flow of actual rivers. Besides, the diameter of a vortex formed by the flow of CASE-I is about a/2, while that of CASE-J is about a. From this fact, it is concluded that the dimension of the secondary flow is governed by the interval of the roughness elements. Except for difference of the scale ,the turbulent structure of the secondary flow of CASE-I and CASE-J is almost the same. Therefore, the results of CASE-I will be mainly investigated in the following.

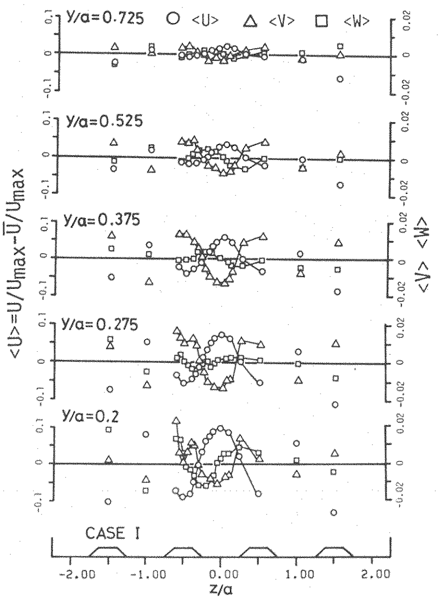

Fig. 5 Spanwise distribution of mean velocity U, V and W

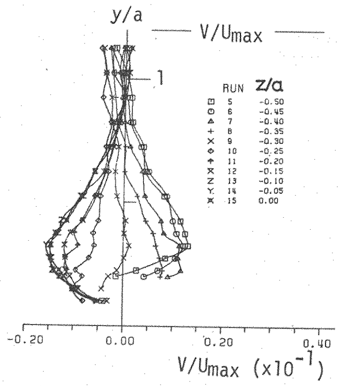

Fig. 6
Vertical distribution of vertical mean velocity V

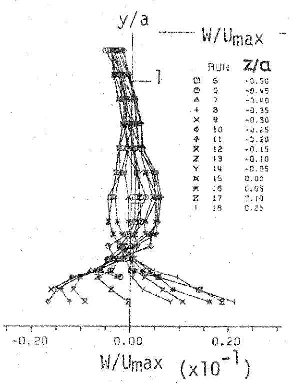

Fig. 7
Vertical distribution of spanwise mean velocity W

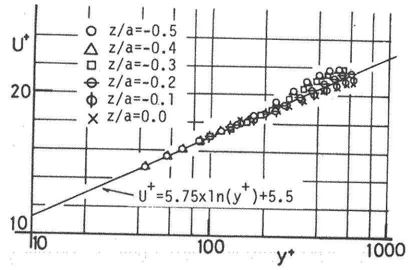

Fig. 8 Distribution of U^+ against y^+

Fig. 5 shows the distribution of U, V and W along the spanwise direction at different heights. The values from which the average over the spanwise direction at each height has been subtracted are plotted in the figure and the values are expressed as < >, i.e. <U>. The origin of y/a is taken on the bottom of trough bed. Except for the region where the measured point is sparse and <V> near the wall, all values vary sinusoidally. The phase of <V> lags about 180° behind <U> and that of <W> lags 90°.

Figs. 6 and 7 show the vertical distributions of V and W, respectively. These figures show that V tends to approach to zero near the wall, and it has the maximum value at $y/a = 0.25$ where the center of the secondary vortex exists, and it decreases toward the center of the channel. W is zero about $y/a = 0.25$ and changes the sign from positive to negative or reversely at this point. The values of W in the lower region($y/a < 0.25$) is larger than those in the upper region($y/a > 0.25$). So, it is known that the secondary flow forms a little one-sided vortex which has rapid flow near the wall and slow and broad flow in the upper side.

The vertical distribution of U is next examined. As the position of the bottom changes in z-direction in this experiment, the origin of y-coordinate is taken on the bottom at each spanwise position and the height from this origin is expressed in terms of y'. Fig. 8 shows the distribution of U^+ ($\equiv U/U_*$) against y^+ ($\equiv U_* y'/\nu$) plotted on semi-logarithmic graph, and the solid line in the figure indicates the log-law which is given by the following equation:

$$U/U_* = 5.75\ \log_{10}(U_* y'/\nu) + 5.5 \qquad (1)$$

where U_* is the local friction velocity. In the inner region where $y^+ < 250$, U^+ agrees well with this log-law both in the ridge and the trough areas. But, in the outer region where $y^+ > 250$, the value of U^+ on the ridge area becomes larger than Eq. 1 and that on the trough area becomes smaller. These are caused by the fact that the friction velocity U_* is different from point to point in spanwise direction.

Fig. 9 shows the distribution of U_* in spanwise direction. These values of U_* have been estimated by applying the log-law to the measured velocity distributions. U_* becomes smaller on the ridge area and larger on the trough area. Thus, U_* becomes smaller in upflow region and larger in downflow region when the secondary flow exists. In other words, U in the region $y^+ < 250(y'/a < 0.4 \sim 0.5)$ where the log-law is applicable is decelerated on the ridge area and is accelerated on the trough area.

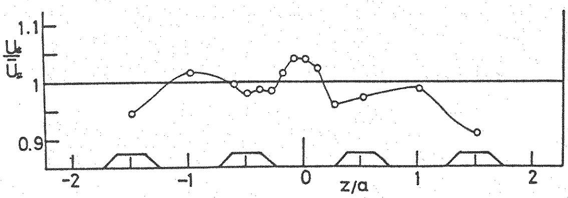

Fig. 9 Spanwise Distribution of local fliction velocity U_*

In Fig. 10, the spanwise distribution of turbulence intensities of three components <u'>, <v'> and <w'> are shown. Each component of turbulence intensity shows similar trend of the distribution such that the value in the ridge area is larger than that in the trough area. By careful inspection, it is recognized that <u'> and <v'> near the wall tend to become smaller on the ridge than those on the trough, but <w'> does not. As for the amplitude of the variation, the relationship that $u' > w' > v'$ is generally recognized, but their mabnitudes become almost equal near the central part of the channel.

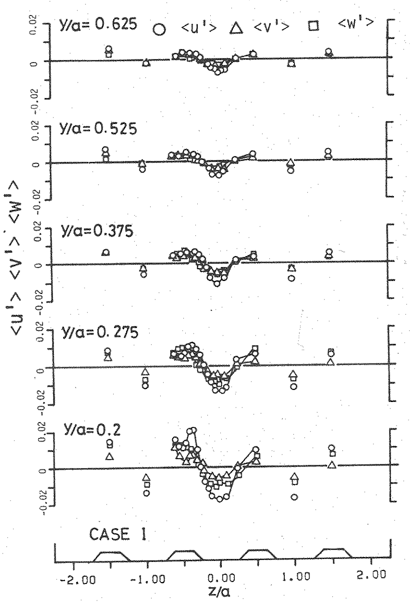

Fig. 10 Spanwise distribution of turbulence intensities <u'>, <v'> and <w'>

Fig. 11 shows the vertical distribution of u'. The thick solid line in this figure indicates the distribution on the uniform smooth bed of CASE-H. In comparison with this line, the values in CASE-I lie above this line in the ridge area and below the line in the trough area. Consequentry, it is concluded that theturbulence intensity cannot be expressed universally in terms of U_* obtained from the log-law. This is explained in the following manner: in the ridge area, high turbulent fluid in the lower layer is carried upward by upflow, while in the trough area, low turbulent fluid in the upper layer is carried downward by downflow. The distribution of v' and w' in vertical direction is almost similar to that of u'.

Fig. 12 shows the spanwise distributions of $<-\overline{uv}>$ and $<-\overline{uw}>$. The distribution of $<-\overline{uv}>$ is similar to that of turbulence intensity and shows a sinusoidal undulation of which amplitude is larger in the ridge area and smaller in the trough area. The distribution of $<-\overline{uw}>$ lags in phase from that of $<-\overline{uv}>$, i.e. it has a maximum on the right-side of the ridge and has a minimum on the left-side. The amplitude of the variation of $<-\overline{uw}>$ is almost two times larger than that of $<-\overline{uv}>$ with a sharp peak.

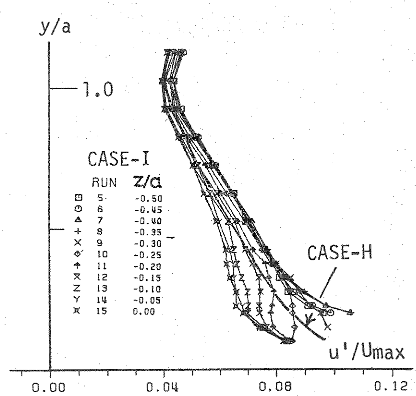

Fig. 11 Vertical distribution of turbulence intensity u'

Figs. 13 and 14 show the vertical distributions of $-\overline{uv}$ and $-\overline{uw}$, respectively. The thick solid line in Fig. 13 indicates the linear distribution in CASE-H. The values of $-\overline{uv}$ in the ridge area are located above this line and those

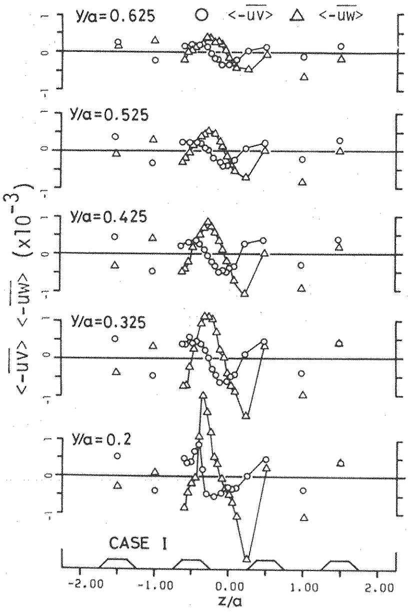

Fig. 12 Spanwise distribution Of Reynolds stress $<\overline{-uv}>$ and $<\overline{-uw}>$

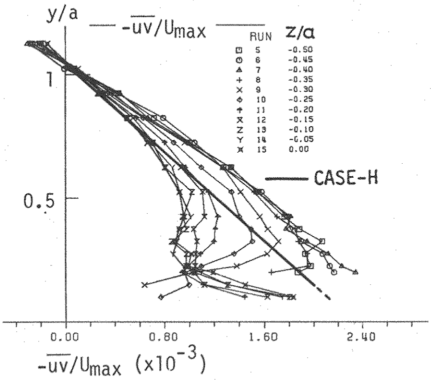

Fig. 13 Vertical distribution of Reynolds stress $\overline{-uv}$

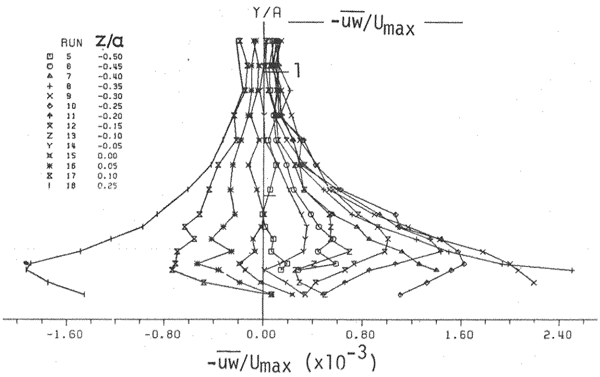

Fig. 14 Vertical distribution of spanwise Reynolds stress $\overline{-uw}$

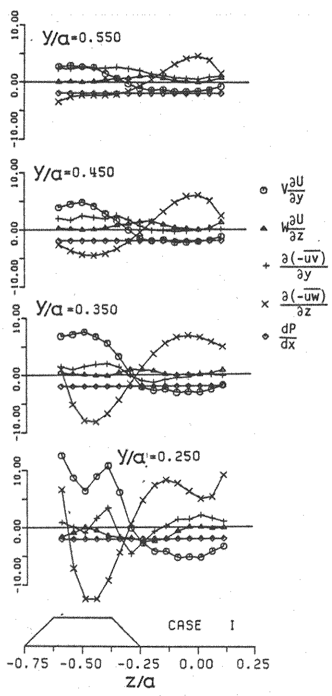

Fig. 15 Spanwise distribution of the terms of equation of motion

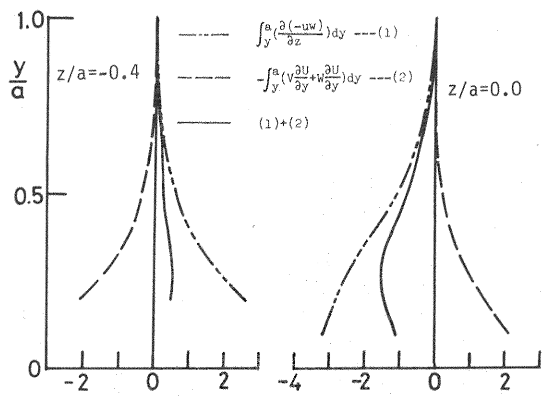

Fig. 16 Distribution of additional stresses with secondary flow on the ridge and trough

in the trough area show a characteristic distribution which is considerably small in the lower part and is constricted in the middle. The value of $-\overline{uw}$ is almost zero at the center of both the ridge and the trough, and it is positive on the right-side of the ridge and negative on the left-side.

EXAMINATION OF EQUATION OF MOTION

In this section, the changes of the turbulent structure due to secondary flow will be examined by order estimation of each term of the equation of motion using the present experimental data. Equation of motion in the x-direction is given as follows :

$$V\frac{\partial U}{\partial y} + W\frac{\partial U}{\partial z} = -\frac{1}{\rho}\frac{dP}{dx} - \frac{\partial(\overline{uv})}{\partial y} - \frac{\partial(\overline{uw})}{\partial z} + \nu\frac{\partial^2 U}{\partial y^2} + \nu\frac{\partial^2 U}{\partial z^2} \qquad (2)$$

where P is wall pressure. Fig. 15 shows the spanwise distribution of each term in Eq. 2. Only the term of dP/dx was not measured spanwisely, but this term can be assumed constant in spanwise direction(from the differenciation of the z-direction equation of motion with respect to x, $\partial/\partial x(\partial P/\partial z) = 0$ and so $\partial/\partial z(\partial P/\partial x) = 0$). Besides, the viscous term $\nu\partial^2U/\partial y^2 + \nu\partial^2U/\partial z^2$ can be neglected in comparison with other terms except for very near the wall. From Fig. 15, the followings are recognized : although the value of $\partial(-\overline{uw})/\partial z$ is negative in the ridge area and positive in the trough area, its absolute value is largest throughout the flow depth and balances with the value of $V\partial U/\partial y$. In the boundary region, the value of $W\partial U/\partial z$ appears. The value of $\partial(-\overline{uv})/\partial y$ undulates in spanwise direction near the wall, but this becomes constant far from the wall.

By integrating Eq. 2 for y, the following equation is obtained :

$$-\overline{uv} + \nu\frac{\partial U}{\partial y} = \left(-\frac{1}{\rho}\frac{dP}{dx}\right) a \left(1 - \frac{y}{a}\right) + \int_y^a \frac{\partial(-\overline{uw})}{\partial z}dy - \int_y^a \left(V\frac{\partial U}{\partial y} + W\frac{\partial U}{\partial z}\right) dy \qquad (3)$$

The first term of the righthand side in Eq. 3 represents a linear distribution without the secondary flow. The second and third terms indicate the effect of the secondary flow on the distribution of $-\overline{uv}$. Fig. 16 shows the latter two integrated values and the sum of them both in the ridge and the trough areas. In the ridge area, this sum is positive, i.e. $-\overline{uv}$ increases, while in the trough area, this sum is largely negative, i.e. $-\overline{uv}$ decreases. The result reasonably explains the distribution of $-\overline{uv}$ shown in Fig. 12. If y is taken as zero in Eq. 3, the lefthand side in Eq. 3 is equal to U_*^2. Since U_* obtained from log-law was small on tha ridge area and large on the trough area, it seems to bring about a result opposite to that of Fig. 16. But, it is supposed that these additional stress terms change the sign from positive to negative or reversely very near the wall.

CONCLUSION

In the present study, the turbulent structures of the flow with cellular secondary flow have been investigated by experiment. By placing the roughness elements with trapezoidal cross section on the bed, the secondary flow has been produced so that the upflow appears on the ridge area and the downflow on the trough. It has been recognized from the experimental results that the main flow velocity is smaller and the turbulence intensities and the Reynolds stress are larger in upflow region than those in downflow region. And, the spanwise Reynolds stress $-\overline{uw}$ reveals a predominant effect on the structure of the flow with the secondary flow. In this case, it is considered that the arrangement, width, height and shape of the roughness elements play an impotant role on the producing mechanism of the secondary flow. Further investigation on this point is needed.

Most of this paper is translated from the authors' Japanese paper (5), but partly modified.

REFERENCES

1. Allen, J.R.L. : Some sedimentary structures, and a note on texture and fabric, Physical processes of sedimentation, George Allen and Unwin LTD, London, 1977.
2. Karcz, I. : Secondary currents and the configulation of a natural stream bed, Journal of Geophysical Research, Vol.71, pp.3109 - 3116, 1966.
3. Nakagawa, H., I. Nezu and A. Tominaga : Turbulent structure with and without cellular secondary currents over various bed configulations, Annual Bulletin of the Disaster Prevension Research Institute, Kyoto University, Vol.24 B-2, pp.315 - 338, 1981.
4. Nakagawa, H., I. Nezu and A. Tominaga : The turbulent structure of the cellular secondary currents in a straight duct, Japanese 13th Symposium of Turbulence, Tokyo University, 1981.
5. Nakagawa, H., I. Nezu and A. Tominaga : Turbulent structure with secondary flow, Proc. of 25th Japanese Conference on Hydraulics, pp.469-474, 1982.

APPENDIX - NOTATION

The following symbols are used in this paper :

a	= a half of the channel height;
P	= wall pressure;
U, V, W	= mean velocity parallel to x, y, z directions, respectively;
U_{max}	= mean velocity parallel to x direction at the center of the duct (z=0, y=a);
U^+	= U/U_*;
U_*	= friction velocity;
u, v, w	= instantaneous values of velocity fluctuations parallel to x, y, z directions,respectively;
$\tilde{u}, \tilde{v}, \tilde{w}$	= instantaneous values of velocity parallel to x, y, z directions, respectively;
u', v', w'	= root-mean-square of velocity fluctuations u, v, w, respectively;
$-\overline{uv}$	= component in x-y plane of Reynolds stress tensor;
$-\overline{uw}$	= component in x-z plane of Reynolds stress tensor;
x	= longitudinal coordinate along duct;
y	= vertical coordinate (y=0 corresponds to the bottom of trough area);
y^+	= $U_* y/\nu$;
y'	= vertical coordinate (y'=0 corresponds to the bottom at each spanwise position);
z	= lateral coordinate (z=0 corresponds to duct center line);
ν	= kinematic viscosity; and
$< >$	= the values from which the average over the spanwise direction at level y is subtracted.